Spectroscopy of GaAs/AlGaAs quantum-cascade lasers using hydrostatic pressure

S. R. Jin, C. N. Ahmad, S. J. Sweeney, A. R. Adams, and B. N. Murdin
Advanced Technology Institute, University of Surrey, Guildford, Surrey GU2 7XH, United Kingdom

H. Page,[a] X. Marcadet, and C. Sirtori
Thales Research and Technology, Technological Platform, Domaine de Corbeville, 91404 Orsay, France

S. Tomić[b]
Computational Science and Engineering Department, CCLRC Daresbury Laboratory, Warrington, Cheshire WA4 4AD, United Kingdom

(Received 31 May 2006; accepted 4 September 2006; published online 27 November 2006)

The authors have measured the output spectrum and the threshold current in 9.2 μm wavelength GaAs/$Al_{0.45}Ga_{0.55}As$ quantum-cascade lasers at 115 K as a function of hydrostatic pressure up to 7.3 kbars. By extrapolation back to ambient pressure, thermally activated escape of electrons from the upper lasing state up to delocalized states of the Γ valley is shown to be an important contribution to the threshold current. On the other hand leakage into the X valley, although it has a very high density of states and is nearly degenerate with the Γ band edge in the barrier, is insignificant at ambient pressure. © *2006 American Institute of Physics*. [DOI: 10.1063/1.2364159]

Since the realization of the GaAs-based quantum-cascade laser (QCL),[1] an impressive extension of the attainable infrared frequency range has been achieved. It can operate at wavelengths as long as 160 μm,[2] or in dual frequency regime up to 215 μm.[3] The design of GaAs/AlGaAs QCLs can be made very flexible by varying the Al content due to naturally occurring near lattice matched material system across the full range of Al contents. Hence, following the terahertz emitting QCL,[4] several laser designs based on 15% Al content in the barriers were presented, approaching high temperature pulsed operation[5] or close to liquid nitrogen temperature cw operation.[6] GaAs-based QCLs emitting in the midinfrared (MIR) spectral region have so far used Al contents of 33%,[1] 45%,[7–9] and 100%,[10–12] respectively, and have been subjected to a high external magnetic field.[13] Pulsed room temperature operation has been reported only for designs with 45% Al content[7–9] and for a hybrid GaAs/InAs/AlAs design.[11] Achieving cw operation in MIR GaAs-based QCLs is a very challenging task due to the relatively high threshold current densities (I_{th}). Influence of the injector doping,[14] the lattice temperature,[15] and carrier escape via weakly localized Γ states[16] were attributed as major limiting factors, for the high temperature operation and attainable gain, that determine the increase of I_{th} and dynamic working range of ~9 μm GaAs-based QCLs. Nevertheless, cw operation has been reported[10,17] with operating temperatures up to 150 K. However, the output characteristics are still inferior compared to InP MIR QCL.[18] Apart from Γ-band related scattering, particularly in AlAs material, the importance of Γ-X transport processes was examined in detail.[19,20] Recently, in the Sb-based QCLs the Γ-X intervalley scattering is attributed as a possible limiting factor for the emission shorter than ~4 μm.[21]

The temperature sensitivity of the GaAs/$Al_xGa_{1-x}As$ QCL's I_{th} decreases as the Al content increases from 33% to 45% in the barrier region. This is attributed to the increase in the activation energy for thermal escape[12] of electrons from the quantum well into the upper Γ miniband of the injector, which reduces its magnitude. However, at high Al concentrations the participation of lateral X and L valleys is believed to be an important factor deteriorating the device performance due to the near degeneracy with the Γ conduction band edge at x=45% in the barrier.[22] A key to the correct design of QCLs is the incorporation of a minigap in the injector states at the energy of the upper lasing level (E_3), which increases the upper state lifetime and reduces leakage. However, in GaAs/AlGaAs devices the bottom of the next miniband above E_3 is close in energy, and recent work[7,12] reveals the importance of thermally activated escape of electrons through this upper Γ miniband. Time-resolved experiments have shown that Γ-Γ is faster than Γ-X scattering in spite of the increased density of states in the X valley.[23] It is crucial to identify the relative importance of different scattering mechanisms to the injection current of the QCL. The externally applied high pressure is a very useful tool because it tunes the Γ-X and Γ-L separations in a controlled manner, within a single structure. It may therefore be used as a means of differentiating between these different current channels and the extent to which they contribute to the I_{th} under ambient conditions, due to the fact that each current channel has a different pressure dependence.

In this letter, we report high-pressure studies of GaAs/$Al_{0.45}Ga_{0.55}As$ QCL measured at 115 K. The devices emit at ~9 μm and were grown by molecular beam epitaxy on a heavily n-doped GaAs substrate. They have a standard structure with a "diagonal" transition across three coupled quantum wells. The details of the growth and fabrication procedure of the devices can be found in previous work.[7,12] The lasers were processed with ridges 30 μm wide, cleaved into chips with a cavity length of 2 mm and mounted unbonded in a spring clip that provided electrical and thermal contact. The clip was inside an optical pressure cell, which was in turn in a vacuum, clamped to the underside of a cryostat's nitrogen bath. The cell was connected to a helium

[a]Present address: TeraView Ltd., Platinum Building, St. John's Innovation Park, Cowley Road, Cambridge CB4 0WS, UK.
[b]Electronic mail: s.tomic@dl.ac.uk

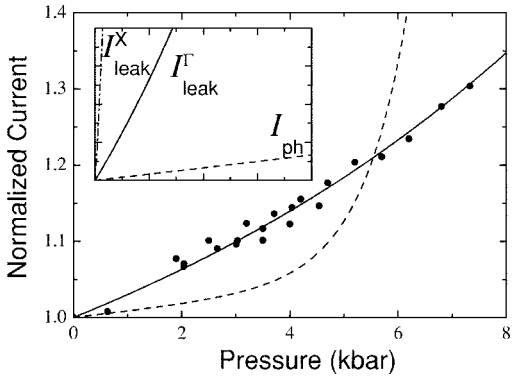

FIG. 1. Normalized I_{th} in a GaAs/$Al_{045}Ga_{0.55}As$ quantum-cascade laser at 115 K, measured experimentally as a function of hydrostatic pressure (circles). Inset (same axes as main figure): calculated normalized pressure dependence of three current pathways out of the upper laser state (leakage through the barrier X states and through barrier Γ states and intersubband relaxation via optical phonon scattering data). Also shown in the main figure are fits to the observed pressure dependence of the I_{th} using different combinations of the three current channels from the inset: ignoring X leakage (solid line) gives a good fit and $I_{th}=0.81I_{ph}+0.19I^{\Gamma}_{leak}$; ignoring Γ leakage (dotted line) gives a poor fit and $I_{th}=0.9998I_{ph}+0.0002I^{X}_{leak}$.

gas compressor and the system can generate pressures up to 10 kbars (1 GPa). The temperature was measured using a thermocouple on the outer surface of the pressure cell, which had been previously calibrated using a buried thermocouple inside the pressure cell. The measurements were performed under pulsed operation (50 ns pulse width at a repetition frequency of 2 kHz), thereby minimizing current heating effects. Light was collected outside the cell through silicon windows.

Figure 1 displays the pressure dependence of the threshold current density. The figure includes a combination of data taken as the pressure was increased and reduced back down to 1 atm, showing that the pressure effect is reversible. It was found that J_{th} increased with increasing pressure by 30% over a 7.3 kbar pressure range. The emission spectrum was also measured, slightly above threshold, using an interferometer having a 1 cm^{-1} resolution. A linear shift to longer wavelength was observed with a pressure coefficient of the transition energy $d(h\nu)/dP=-0.417$ meV/kbar as shown in Fig. 2. The very small tuning in the lasing transition energy

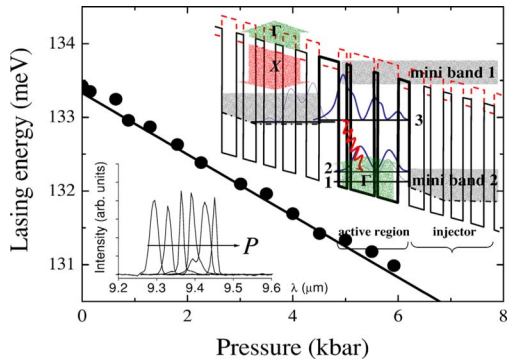

FIG. 2. (Color online) Pressure dependence of the laser emission energy. Insert bottom left: spectra taken at $P=0$, 1.3, 2.3, 3.5, 4.0, and 5.5 kbars with 1 cm^{-1} resolution Fourier transform infrared. Insert top right: Schematic diagram of the band structure in a GaAs/AlGaAs quantum-cascade device. The dotted line is the X-valley minimum, and "mini-1" and "mini-2" are the lower and upper minibands of the injector/collector region, respectively. The length and direction of the arrows indicate the direction and relative size of the pressure tuning.

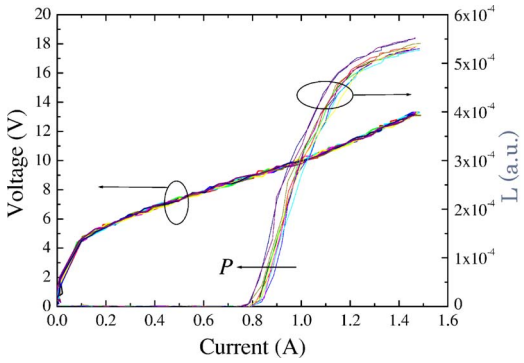

FIG. 3. (Color online) Pressure dependence of the measured L-I-V characteristics at 115 K taken in the range of $P=0$ to $P=5.5$ kbars.

is indicative that the positions of the energy levels in the active region do not change significantly. This is consistent with the measured L-I-V characteristics at different pressures, Fig. 3, which show that the applied voltage is also approximately independent of pressure (within ±2%). Our modeling shows that even with changes in electric field, the dipole matrix element $\langle z_{32}\rangle$ stays practically constant. Consequently we assume that the electric field at threshold can be considered constant in the pressure range used, and the main effect of pressure is to change the lifetime $\tau_3^{th}=1/(1/\tau_{31}^{ph}+1/\tau_{32}^{ph}+1/\tau_{leak}^{\Gamma})$. The laser mirror loss is independent of pressure due to the negligible change of the refractive index of the medium over the experimental pressure range. Therefore, we only consider pressure-induced changes in electronic band structure and transition rates. The effects of pressure on band structure that are important for electrons in the conduction band of a GaAs/AlGaAs heterostructure (see Fig. 2 insert) are (a) reduction of the separation between the Γ and X conduction band edge energies at $dE^{\Gamma,X}/dP\sim-13.5$ meV/kbar, (b) increase of the separation between the Γ and L conduction band edges at $dE^{\Gamma,L}/dP\sim2$ meV/kbar, (c) decrease slightly of the Γ-Γ band offset due to the difference in pressure coefficients of the two materials at $dE^{\Gamma,\Gamma}/dP\sim-1.2$ meV/kbar, and (d) blueshift of the Γ band gap at $dE_g/dP\sim10$ meV/kbar. The pressure variation of the various band edges in the well or barrier material at the Γ point was estimated from $dE^{\Gamma}_{g(CB)}/dP=-3a_{g(CB)}/(c_{11}+2c_{12})$, where $a_{g(CB)}$ is the energy gap (conduction band) deformation potential and c_{ij} are elastic constants,[24] while at the X point $dE^{X}_{CB}/dP=-0.8$ meV/kbar.[25]

Because the Γ-L separation increases with pressure, if leakage through L were important the I_{th} would decrease. This is counter to our observation (Fig. 1) and hence we discount this current path. We therefore assume that the pressure-induced changes occur mainly in the relative positions of the Γ and X states in the heterostructure. At the highest pressure studied, which corresponds to near degeneracy of the barrier X valley with the upper lasing state, one might expect considerable influence of this valley (though, as shown below this is not the case).

The change in band gap (corresponding to a 5% blueshift over the experimental pressure range) produces a proportional increase in the electron effective mass m^* at the Γ point according to the Kane model, and hence also a redshift in the intersubband quantization energy.[26] The calculated tuning of the energy levels according to an eight-band $\mathbf{k}\cdot\mathbf{P}$ envelope function model (i.e., including nonparabolicity) for

a fixed electric field of 48 kV/cm is shown in Fig. 2. This shows excellent agreement with the experiment. The pressure tuning of the lasing wavelength is rather smaller (3% over the experimental pressure range) than the change in band-edge effective mass (5%). The small change in emission wavelength and the invariant *I-V* characteristics (see Fig. 3) suggest that the alignment of the QCL structure, so critical to its operation, is virtually unchanged over the pressure range measured.

The total threshold current may be written as $I_{\mathrm{th}}=I_{\mathrm{ph}}+I^{\Gamma}_{\mathrm{leak}}+I^{X}_{\mathrm{leak}}$. $I_{\mathrm{ph}}\propto 1/[\Delta E_{32}\langle z_{32}\rangle^2\tau_3^{\mathrm{ph}}(1-\tau_2^{\mathrm{ph}}/\tau_{32}^{\mathrm{ph}})]$ is the nonradiative current due to optical phonon scattering, where $\tau_3^{\mathrm{ph}}=1/(1/\tau_{31}^{\mathrm{ph}}+1/\tau_{32}^{\mathrm{ph}})$ and $\tau_2^{\mathrm{ph}}\approx\tau_{21}^{\mathrm{ph}}$. The longitudinal optical phonon scattering times are proportional to[27]

$$\frac{1}{\tau_{ij}^{\mathrm{ph}}}\propto\int\frac{|\langle i|\exp(-iq_z z)|j\rangle|^2}{\sqrt{(\hbar^2k_{\parallel}q_z/m^*)^2+(\hbar^2q_z^2/2m^*+E_i-E_j-\hbar\omega_{\mathrm{LO}})^2}}dq_z, \tag{1}$$

where E_j and $|j\rangle$ are the jth confined state and its wave function, $\hbar\omega_{\mathrm{LO}}$ is the energy of the emitted longitudinal optical phonon, $\langle i|\exp(-iq_z z)|j\rangle$ is the overlap integral taking into account interface effects, q_z is the LO phonon wave vector along the growth direction, and m^* is the in plane electron effective mass. From Eq. (1) one can make the approximation $\tau_{32}^{\mathrm{ph}}\propto 1/m^*(P)$. The carrier leakage through the upper manifold of Γ states and through the X valley, $I^{\Gamma}_{\mathrm{leak}}$ $(\propto 1/\tau^{\Gamma}_{\mathrm{leak}})$ and $I^{X}_{\mathrm{leak}}(\propto 1/\tau^{X}_{\mathrm{leak}})$, respectively, are determined by the corresponding escape times, $\tau^{\Gamma}_{\mathrm{leak}}$ and τ^{X}_{leak}, and can be described by $\tau^{\Gamma,X}_{\mathrm{leak}}=(k_BT/2\pi m^*)^{1/2}\exp[-(\Delta E^{\Gamma,X}_{\mathrm{act}}/k_BT)]/l$,[28] where $\Delta E^{\Gamma,X}_{\mathrm{act}}$ is the activation energy into the Γ or X levels, k_BT is the thermal energy, and l is the spatial extent of the wave function of the upper laser level, $\sim$100 Å in these devices. Since the upper Γ-miniband states have most of their weight in the continuum, their energy follows the barrier Γ band edge and this leads to a slight reduction of $\Delta E^{\Gamma}_{\mathrm{act}}$. The Γ and X valleys of the barrier material are degenerate at ambient pressure, so the initial activation energies $\Delta E^{\Gamma,X}_{\mathrm{act}}$ to the Γ and X states are nearly identical. While only a slight variation in $\Delta E^{\Gamma}_{\mathrm{act}}$ is expected with pressure, $\Delta E^{X}_{\mathrm{act}}$ is expected to change by $\sim$80% over the experimental pressure range. The calculated normalized pressure dependence of the three respective current components is displayed in the inset of Fig. 1. It shows that I_{ph} remains fairly constant over the pressure range considered. $I^{\Gamma}_{\mathrm{leak}}$ increases significantly, while I^{X}_{leak} shows the most rapid increase. Figure 1 displays fits to the experiment using the different combinations of the above three current components: either ignoring Γ leakage or ignoring X leakage. It shows that $I_{\mathrm{ph}}/I_{\mathrm{th}}|_{P=0}=81\%$ and $I^{\Gamma}_{\mathrm{leak}}/I_{\mathrm{th}}|_{P=0}=19\%$ (solid line) gives a good fit to the experimental data over the pressure range considered. We observed considerably bigger Γ leakage than previously predicted[29] for the same QCL structure.[7] Current leakage via Γ-X transitions is negligible in the pressure range we studied. This is consistent with previous measurements of the temperature dependence and barrier height dependence of I_{th} where it was found that nonradiative current via optical phonon scattering dominates I_{th} at low temperature while carrier leakage into the Γ miniband is responsible for the temperature dependence of the devices at higher temperatures.[12]

In summary, in order to understand the origin of I_{th} in $GaAs/Al_{0.45}Ga_{0.55}As$ QCL, an experimental and theoretical study of its pressure dependence has been reported. The positions of the energy levels in the QCL's active region do not change significantly over the pressure range considered but separation between Γ and X band edges can be tuned. We conclude that the relative contributions from LO phonon scattering in Γ band and Γ leakage to the I_{th} are approximately in the ratio 4:1, whereas X leakage is less than 0.03% and consequently negligible in this particular design.

The authors would like to thank D. Indjin and G. J. Strudwick for useful discussions. This work was supported by the UK-EPSRC (GR/R19298/01).

[1] C. Sirtori, P. Kruck, S. Barbieri, P. Collot, J. Nagle, M. Beck, J. Faist, and U. Oesterie, Appl. Phys. Lett. **73**, 3486 (1998).
[2] G Scalari, S. Blaser, J. Faist, H. Beere, E. Linfield, D. Ritchie, and G. Davies, Phys. Rev. Lett. **93**, 237403 (2004).
[3] G. Scalari, C. Walther, J. Faist, H. Beere, and D. Ritchie, Appl. Phys. Lett. **88**, 141102 (2006).
[4] R. Kohler, A. Treducucci, F. Beltram, H. E. Beere, E. H. Linfield, A. G. Davies, D. A. Ritchie, R. C. Iotti, and F. Rossi, Nature (London) **417**, 156 (2002).
[5] S. Kumar, B. S. Williams, S. Kohen, Q. Hu, and J. L. Reno, Appl. Phys. Lett. **84**, 2494 (2004).
[6] S. Barbieri, J. Alton, H. E. Beere, E. H. Linfield, and D. A. Ritchie, Appl. Phys. Lett. **85**, 1674 (2004).
[7] H. Page, C. Becker, A. Robertson, G. Glastre, V. Ortiz, and C. Sirtori, Appl. Phys. Lett. **78**, 3529 (2001).
[8] S. Anders, W. Schrenk, E. Gornik, and G. Strasser, Appl. Phys. Lett. **80**, 1864 (2002).
[9] C. Pflügl, W. Schrenk, S. Anders, G. Strasser, C. Becker, C. Sirtori, Y. Bonetti, and A. Muller, Appl. Phys. Lett. **83**, 4698 (2003).
[10] W. Schrenk, N. Finger, S. Gianordoli, E. Gornik, and G. Strasser, Appl. Phys. Lett. **77**, 3328 (2000).
[11] D. A. Carder, L. R. Wilson, R. P. Green, J. W. Cockburn, M. Hopkinson, M. J. Steer, R. Airey, and G. Hill, Appl. Phys. Lett. **82**, 3409 (2003).
[12] V. Ortiz, C. Becker, H. Page, and C. Sirtori, J. Cryst. Growth **251**, 701 (2003).
[13] A. Leuliet, A. Vasanelli, A. Wade, G. Fedorov, D. Smirnov, G. Bastard, and C. Sirtori, Phys. Rev. B **73**, 085311 (2006).
[14] V. D. Jovanovic, D. Indjin, N. Vukmirovic, Z. Ikonic, P. Harrison, E. H. Linfield, H. Page, X. Marcadet, C. Sirtori, C. Worrall, H. E. Beere, and D. A. Ritchie, Appl. Phys. Lett. **86**, 211117 (2005).
[15] V. Spagnolo, G. Scamarcio, H. Page, and C. Sirtori, Appl. Phys. Lett. **84**, 3690 (2004).
[16] S. Höfling,V. D. Jovanovic, D. Indjin, J.P. Reithmaier, A. Forschel, Z. Ikonic, N. Vukmirovic, P. Harrison, A. Mircetic, and V. Milanovic, Appl. Phys. Lett. **88**, 251109 (2006).
[17] H. Page, S. Dhillon, M. Callgaro, C Becker, V. Ortiz, and C. Sirtori, IEEE J. Quantum Electron. **40**, 665 (2004).
[18] M. Beck, D. Hofstetter, T. Aellen, J. Faist, U. Oesterie, M. Ilegems, E. Gini, and H. Melchior, Science **295**, 301 (2001).
[19] E. Raichev, Phys. Rev. B **49**, 5448 (1994).
[20] J. J. Finley, R. J. Teissier, M. S. Skolnick, J. W. Cockburn, G. A. Roberts, R. Grey, G. Hill, M. A. Pate, and B. Planel, Phys. Rev. B **58**, 10619 (1998).
[21] Q. Yang, C. Manz, W. Bronner, K. Köhler, and J. Wagner, Appl. Phys. Lett. **88**, 121127 (2006).
[22] L. R. Wilson, D. A. Carder, J. W. Cockburn, R. P. Green, D. G. Revin, M. J. Steer, M. Hopkinson, G. Hill, and R. Airey, Appl. Phys. Lett. **81**, 1378 (2002).
[23] S. R. Schmidt, E. A. Bivik, A. Sellmeier, L. E. Vorobiev, A. E Zhukov, and U. M. Ustinov, Appl. Phys. Lett. **78**, 1261 (2001).
[24] I. Vurgaftman, J. R. Meyer, and L. R. Ram-Mohan, J. Appl. Phys. **89**, 5815 (2001).
[25] S. Adachi, J. Appl. Phys. **58**, R1 (1985).
[26] Z. Wasilewski and R. A. Stradling, Semicond. Sci. Technol. **1**, 264 (1986); R. J. Warburton, M. Watts, R. J. Nicholas, J. J. Harris, and C. T. Foxon, *ibid.* **7**, 787 (1992).
[27] G. Sun and J. B. Khurgin, IEEE J. Quantum Electron. **29**, 1104 (1993).
[28] H. Schneider and K. V. Klitzing, Phys. Rev. B **38**, 6160 (1988).
[29] D. Indjin, P. Harrison, R. W. Kelsall, and Z. Ikonić, Appl. Phys. Lett. **81**, 400 (2002).